

# Magnitudes and Sources of Dissolved Inorganic Phosphorus Inputs to Surface Fresh Waters and the Coastal Zone: A New Global Model

## *Authors*

John A. Harrison, Lex Bouwman, Emilio Mayorga, Sybil Seitzinger

John A. Harrison  
Washington State University  
School of Earth and Environmental Sciences  
14204 NE Salmon Creek Avenue  
Vancouver, WA 98686  
Phone: (360)546-9210  
Fax: (360)546-9064  
Email: [harrisoj@vancouver.wsu.edu](mailto:harrisoj@vancouver.wsu.edu)

A. F. (Lex) Bouwman  
Netherlands Environmental Assessment Agency (PBL)  
PO Box 303  
3720 AH Bilthoven  
The Netherlands  
Email: [Lex.Bouwman@pbl.nl](mailto:Lex.Bouwman@pbl.nl)

Emilio Mayorga  
Applied Physics Laboratory  
University of Washington  
Box 355640  
Seattle, WA 98105-6698 USA  
Email: [mayorga@apl.washington.edu](mailto:mayorga@apl.washington.edu)

Sybil P. Seitzinger  
Sybil Seitzinger (IGBP, Stockholm – also LME associated)  
IGBP-Royal Swedish Academy of Sciences  
Box 50005  
104 05 Stockholm, Sweden  
Email: [sybil.seitzinger@igbp.kva.se](mailto:sybil.seitzinger@igbp.kva.se)

## Abstract

As a limiting nutrient in aquatic systems, phosphorus (P) plays an important role in controlling freshwater and coastal primary productivity and ecosystem dynamics, increasing frequency and severity of harmful and nuisance algae blooms and hypoxia, as well as contributing to loss of biodiversity. Although dissolved inorganic P (DIP) often constitutes a relatively small fraction of the total P pool in aquatic systems, its bioavailability makes it an important determinant of ecosystem function. Here we describe, apply, evaluate, and interpret an enhanced version of the Global NEWS-DIP model: NEWS-DIP-Half Degree (NEWS-DIP-HD). Improvements to NEWS-DIP-HD over the original NEWS DIP model include: 1) the preservation of spatial resolution of input datasets at the 0.5 degree level, and 2) explicit downstream routing of water and DIP from half degree cell to half degree cell using a global flow-direction representation. NEWS-DIP explains 78% and 62% of the variability in per-basin DIP export (DIP load) for USGS and global stations, respectively, similar to the original NEWS-DIP model and somewhat more than other global models of DIP loading and export. NEWS-DIP-HD output suggests that hot spots for DIP loading tend to occur in urban centers, with the highest per-area rate of DIP loading predicted for the half-degree grid-cell containing Tokyo ( $6,366 \text{ kg P km}^{-2} \text{ yr}^{-1}$ ). Furthermore, cities with populations  $>100,000$  accounted for 35% of global surface water DIP loading while covering less than 2% of global land surface area. NEWS-DIP-HD also indicates that humans supply more DIP to surface waters than natural weathering over the majority (53%) of the Earth's land surface, with a much larger area dominated by DIP point sources than non-point sources (52% versus 1% of the global land surface, respectively). NEWS-DIP-HD also suggests that while humans had increased DIP input to surface waters more than 4-fold globally by the year 2000, human activities such as dam construction and consumptive water use have somewhat moderated the effect of humans on P transport by preventing (conservatively)  $0.35 \text{ Tg P yr}^{-1}$  ( $\sim 20\%$  of P inputs to surface waters) from reaching coastal zones globally.

## 1. Introduction

Global budgeting efforts suggest that P mining and subsequent use as fertilizer has more than doubled P inputs to the environment over natural, background P from weathering [Mackenzie *et al.*, 1998; Bennett *et al.*, 2001; Fixen and West 2002]. Often a limiting nutrient in lakes and other freshwater systems, P is also thought to play an important role in controlling coastal primary productivity and ecosystem dynamics, increasing frequency and severity of harmful and nuisance algae blooms [Anderson *et al.*, 2002] and hypoxia [Diaz and Rosenberg, 2008], among other effects. Though coastal systems are typically thought of as nitrogen (N)-limited, there are several coastal systems where P-limitation has been demonstrated for at least part of the year [Harrison *et al.*, 1990; Jensen *et al.*, 1998; Fisher *et al.*, 1999; Murrell *et al.*, 2002; Sylvan *et al.*, 2005; Conley *et al.*, 2009], and coastal P-limitation may well become more prevalent if anthropogenic N mobilization increases faster than P mobilization, with projected increases in food and energy production [Justic *et al.*, 1995; Turner *et al.*, 2003].

In many systems dissolved inorganic P (DIP) (also called soluble reactive phosphorus (SRP) or orthophosphate ( $\text{PO}_4^{3-}$ )) constitutes a relatively small portion of the phosphorus in rivers ( $\sim 1.5 \text{ Tg P yr}^{-1}$  transported as DIP globally versus  $\sim 20 \text{ Tg P yr}^{-1}$  as total P (TP) globally [Meybeck, 1982; Melack, 1995]). However, whereas all of the DIP pool is generally thought to be bioavailable in rivers, lakes, and coastal waters, significant portions of the particulate and organic P pools are not available for use by organisms [Bradford and Peters, 1987; Ekholm, 1994; Fox 1989]. Therefore, even accounting for desorption of sorbed P in estuaries [Froelich, 1988; Howarth *et al.*, 1995] DIP plays an important role in controlling the biology of such systems. As such the development of a

DIP loading and river transport model constitutes a critical first step towards a synthetic understanding of coastal P delivery, which must eventually also include models for delivery of particulate and dissolved organic P.

There have been a number of attempts to model within-basin P dynamics at scales ranging from a single catchment [Baffaut *et al.*, 2009] to a large river basin [USGS-SPARROW: Alexander *et al.*, 2008], to studies that include several mid-sized basins [Thieu *et al.*, 2009]. However, until now global-scale P transport models have been limited to predicting P export at the mouths of large river basins as a function of basin-averaged characteristics [e.g. Caraco 1995; Smith *et al.*, 2003; Harrison *et al.*, 2005] or in a non-spatially explicit manner altogether [e.g. MacKensie *et al.*, 1998]. In the sections that follow, we describe, apply, evaluate, and interpret output from an enhanced version of the Global NEWS-DIP model [Harrison *et al.*, 2005]: NEWS-DIP-**Half Degree** (NEWS-DIP-HD).

## **2. Methods**

### ***2.1. NEWS-DIP-HD Description***

NEWS-DIP-HD constitutes an update and modification of the original NEWS-DIP model, which is described in detail in Harrison *et al.* [2005]. As with NEWS-DIP, NEWS-DIP-HD predicts average annual DIP export values, and the central equation of NEWS-DIP-HD is identical to that of the updated NEWS-DIP model (NEWS-DIP-II; Mayorga *et al.*, Submitted). The primary difference between NEWS-DIP-HD and NEWS-DIP-II lies in the fact that NEWS-DIP-HD is applied on a per half-degree grid cell basis, rather than at the large basin scale. The central equation for NEWS-DIP-HD is

as follows:

$$DIP = [P_{sew} + P_{det} + (W_{max}/(1+(R/a)^{-b}))] + [L_{max} \cdot (P_{fert} + P_{am} - P_{exp})/(1+(R/a)^{-b})] \quad (1)$$

where  $DIP$  is the local DIP yield ( $\text{kg P km}^{-2} \text{ yr}^{-1}$ ) to surface waters computed for each half-degree cell globally (as opposed to DIP-load ( $\text{kg P basin}^{-1} \text{ yr}^{-1}$ ) or DIP concentration ( $\text{mg P-L}^{-1}$ )).  $DIP$  is calculated as a function of within-cell P sources, which include both point sources and diffuse sources. Point sources are calculated as the sum of P from human sewage ( $P_{sew}$ ) and P from P-based detergents ( $P_{det}$ ). Diffuse sources are calculated as a function of runoff ( $R$ ) ( $\text{m yr}^{-1}$ ), fertilizer P inputs ( $P_{fert}$ ) ( $\text{kg P km}^{-2} \text{ yr}^{-1}$ ), animal manure P inputs ( $P_{am}$ ), P removal by harvest and animal grazing ( $P_{exp}$ ) ( $\text{kg P km}^{-2} \text{ yr}^{-1}$ ), and four calibrated coefficients defining the shape of the runoff response curve for weathering and non-point DIP sources ( $a$ ,  $b$ ,  $W_{max}$ , and  $L_{max}$ —as in *Harrison et al.*, 2005). Diffuse sources were treated as a sigmoid function of runoff, increasing slowly with runoff at low runoff values, more rapidly with runoff at higher runoffs, and topping out at a threshold level in high runoff systems. This sigmoid relationship between runoff and diffuse sources is responsible for the term  $(1/(1+(R/a)^{-b}))$  in NEWS-DIP-HD's central equation. Input variables consisted of spatially explicit,  $0.5^\circ \times 0.5^\circ$  resolution gridded datasets (Table 2). Calibrated coefficients  $a$ ,  $b$ ,  $W_{max}$ , and  $L_{max}$ , were taken directly from the calibration of the NEWS-DIP model (Table 1 in *Mayorga et al.* [Submitted]) and were not recalibrated at the half-degree scale. These coefficients were set to 0.85, 2, 26, and 0.04, respectively. This calibration was achieved using approximately half of the basins (56 rivers) in the original NEWS-DIP calibration and validation dataset [Harrison

et al., 2005]. Calibration was achieved by optimizing the model to attain the highest model efficiency ( $R^2$ ) while maintaining coefficients within observation-based ranges (as in Harrison et al., 2005). Model efficiency (Capital  $R^2$ , not the coefficient of determination ( $r^2$ )) is a metric ranging from 0 to 1 reflecting the degree of fit between measured and modeled values [Nash and Sutcliffe 1970]. When  $R^2 = 1$ , all points fall on the 1:1 line. When  $R^2$  is 0, model error is equal to the variability in the data. Coefficients relating to point source inputs or reservoir retention were not calibrated.

To calculate DIP contributions from individual cells to coastal margins, local DIP yields were multiplied by a cumulative transfer efficiency factor. The cumulative transfer efficiency factor for each cell was calculated as the product of all local downstream transfer efficiencies ( $1-D$  for each half degree, downstream grid cell where  $D$  is the fraction of DIP removed by reservoirs, calculated for each cell according to Harrison et al. [2005] based on the water residence time of the reservoir(s) in that cell) and the ratio  $Q_{act}:Q_{nat}$  for the entire basin (where  $Q_{act}$  is water discharge accounting for human activities such as water extraction and  $Q_{nat}$  is water discharge without the influence of humans). This makes it possible to use NEWS-DIP-HD to predict coastal DIP yield for every half-degree cell. Values for  $Q_{act}:Q_{nat}$  were the same as those used in Harrison et al. [2005], and when not available, were assumed to equal one.

The magnitudes of individual source contributions to local half degree cells were calculated as follows:

$$DIP_{Sew} = H \cdot P_{sw} \quad (2)$$

$$DIP_{Det} = H \cdot P_{det} \quad (3)$$

$$DIP_{Weathering} = (W_{max}/(1+(R/a)^{-b})) \quad (4)$$

$$DIP_{Fertilizer} = 1 - P_{exp}/(P_{fert} + P_{am}) \cdot (L_{max} \cdot P_{fert}/(1+(R/a)^{-b})) \quad (5)$$

$$DIP_{Manure} = 1 - P_{exp}/(P_{fert} + P_{am}) \cdot (L_{max} \cdot P_{am}/(1+(R/a)^{-b})) \quad (6)$$

where  $H$  is population density,  $P_{sw}$  is per-capita delivery of human P effluent to surface waters via sewage,  $P_{det}$  is per-capita delivery of P to surface waters via sewage and other symbols and coefficient values are the same as in Eq. 1 and Appendix A. To calculate coastal contribution, each source was multiplied by the cumulative transfer efficiency from each cell to the coast.

Improvements to NEWS-DIP-HD over the original NEWS DIP model include: 1) the preservation of spatial resolution of input datasets at the 0.5 degree level, 2) explicit downstream routing of water and DIP from half degree cell to half degree cell using a global flow-direction representation [Vörösmarty et al., 2000 and b], 3) the inclusion of detergent P as a potential DIP point source, 4) the explicit use of the surface P balance concept to calculate non-point DIP sources, and 5) the incorporation of more recent input datasets as model drivers (2000 instead of 1995). Several of these enhancements (numbers 3-5) occurred as a result of updating the NEWS-DIP model to run it with Millennium Assessment scenarios [Seitzinger et al., Submitted; this volume], and are described more completely in Mayorga et al., [Submitted], Bouwman et al., [Submitted; this volume], and Van Drecht et al., [In Press; this volume], respectively.

## **2.2. Model Validation Data**

Concentration and water discharge data from 201 globally distributed sites were used to evaluate the predictive power of the NEWS-DIP-HD model (Figures 1 and 2). These data were derived from 4 primary sources, including data used for the calibration and

validation of the original NEWS-DIP model (109 sites; *Harrison et al.*, 2005), the United Nations Global Environment Monitoring System (GEMS) Water (<http://www.gemswater.org/>; 27 sites), the USGS WQN (56 sites; *Alexander et al.*, 1996), and the CAMREX study of the Amazon River (10 sites: *Devol et al.*, 1995; Fig. 1 and Appendix B). These sites encompassed a broad range of basin sizes (5,896 km<sup>2</sup> - 6,112,000 km<sup>2</sup>), a variety of climate types (ranging from tropical to boreal), and both coastal and inland sites (Figure 1). When available, reported basin surface area was used in calculations. However, in certain cases (e.g. with CAMREX and GEMS data) it was necessary to calculate watershed surface area based on STN 6 hydrography (*Vörösmarty et al.*, 2000a and 2000b). All sites were georeferenced to the STN 6 hydrographic network for ease of comparison between measured and modeled P export. Together, the coastal sites included as validation data accounted for 49% of global runoff. DIP load at each site was calculated as the product of mean annual water discharge and flow-weighted mean [DIP] when sufficient data were available (17 cases). When this wasn't possible, median [DIP] (90 cases) or mean concentrations (94 cases) were used. DIP yield for each site (kg P km<sup>-2</sup> yr<sup>-1</sup>) was calculated as load divided by watershed contributing area. For USGS data, only 5<sup>th</sup> order or larger streams were used.

### **2.3. Model Input Data**

Sewage point source P was calculated in a manner similar to *Van Drecht et al.* [In Press, This Volume]. In this method, per-capita excretion of P is calculated at the national level as a function of per-capita income (higher PPP results in higher per-capita P excretion), per-capita P detergent use, P removal efficiency (by sewage treatment), and

sewage connectivity. Country per-capita P excretion rates were spatially disaggregated by multiplying them by population density, averaged at the half-degree scale. One subtle but important difference between the estimate of point source P inputs used in this analysis and the estimate generated in *Van Drecht et al.* [In Press] is that while *Van Drecht et al.*, [In Press] assume that non-urban half-degree cells contribute no point-source P to surface waters, here we assume that an urban fraction of each half-degree cell contributes point source P (where the urban fraction of each cell is equal to the fraction of a country's population that is urban). Anthropogenic non-point source P inputs included fertilizer and manure, but not septic P, and were calculated according to *Bouwman et al.* [Submitted, this volume]. In this method, fertilizer and manure inputs were disaggregated spatially using land-use information and national fertilizer use statistics (FAO 2008). Then a surface P balance was calculated by subtracting the P exported in crop harvest and animal grazing from fertilizer and manure P inputs, to avoid double counting of P inputs.

#### ***2.4. Post-Processing of Model Output***

Regional and global totals of DIP export were calculated as the sum of all grid cells within continents and ocean drainages as defined by the STN6 global half-degree hydrography dataset [*Vörösmarty et al.*, 2000a]. P retention was calculated as locally emitted DIP minus DIP delivered to the coast. This estimate is likely quite conservative as only large dams were used to estimate reservoir storage of DIP and where no consumptive water used data were available, this loss pathway was assumed to be negligible. Also, floodplain and wetland storage are not included explicitly in the model,

and these loss pathways could be significant.

## ***2. 5. Model Evaluation (Model Uncertainty, Sensitivity, and Efficiency)***

Model uncertainty was evaluated by comparing measured and predicted DIP load and yield. Metrics of model error included root mean squared error (RMSE), model efficiency [*Nash and Sutcliffe 1970*], and inter-quartile range (IQR). Model efficiency was calculated using log-transformed model predictions, load, and yield data. RMSE and IQR were determined using untransformed data and predictions. Model error was compared with interannual variability in several rivers for which multiple years of DIP export data were available. Model sensitivity to inputs and coefficients was examined by increasing each model input by 10% and examining the response in model output. Model sensitivities are expressed as percent change in output ( $100 \times \text{new value}/\text{original value}$ ). In addition, to evaluate how critical each model component was to model predictive capacity, individual model components were removed and Nash-Sutcliffe model efficiency was recalculated. Components with little impact on the model had little impact on Nash-Sutcliffe efficiency, whereas removal of critical model components had a large impact on Nash-Sutcliffe efficiency.

Because DIP load and yield data collected by the USGS in the Mississippi River are based on samples collected at least seasonally over multiple years and analyzed using a consistent analytical approach, we viewed these data as potentially higher quality than data from the diverse array of sources contained within the other global datasets included in this analysis, and thus likely a better test for the NEWS-DIP-HD model than data collected from other sources. Because of this, we present a comparison between NEWS-

DIP-HD predictions and USGS data as well as a comparison between NEWS-DIP-HD predictions and all available P export data. For ease of comparison with the original NEWS-DIP model, we also present a comparison between NEWS-DIP-HD predictions and DIP export measurements used in the original NEWS-DIP paper [Harrison *et al.*, 2005].

### **3. Results and Discussion**

#### ***3.1. Model Performance***

NEWS-DIP explains 60% and 50% of the variability in per-area DIP export (DIP-yield) for USGS sites and for all validation sites, respectively, similar to the NEWS-DIP model and somewhat more than other global models of DIP loading and export (Figure 2, Table 2). It explains 78% and 62% of the variability in per-basin DIP export (DIP load) for USGS and global stations, respectively (Table 2).

Despite the reasonably good fit between measured and modeled DIP yield (or load), error on a basin-by-basin scale is considerable. The standard error of log-transformed predictions is 0.42. DIP yield predictions for 58% of basins are within a factor of two of measurement-based estimates, 82% are within a factor of four, and 90% are within one order of magnitude. Error in DIP yield predictions associated with large basins is similar to error associated with relatively small basins. However, absolute error associated with high-yield basins is somewhat greater than error associated with low-yield basins (Figure 2). The range of errors in NEWS-DIP-HD predictions is comparable to or substantially smaller than that for other DIP export models, as indicated by the inter-quartile range and distribution of prediction errors (Table 2).

The error associated with NEWS-DIP is similar in magnitude to the inter-annual variability of DIP yields in several U.S. rivers. For example, the difference between minimum and maximum DIP export years is 5-fold for the Mississippi River and over an order of magnitude for the Potomac River [data from *Alexander et al.*, 1996]. This suggests that NEWS-DIP-HD predictions are likely to fall within the range of inter-annual variability for any given river.

In general, the NEWS-DIP-HD model preserves the spatial resolution of DIP sources and sinks at the 0.5 degree level without sacrificing significant prediction accuracy. In the sections that follow, we use the NEWS-DIP-HD model to gain insight into patterns, controls and sources of DIP export from watersheds worldwide. We then explore model sensitivities, uncertainties, and potential ways to improve our capacity to model DIP export in future efforts.

## **3.2 Model Output**

### ***3.2.1 Spatial Distribution of DIP Export and Sources***

#### *Export*

Comparison of NEWS-DIP-HD output with NEWS-DIP output reveals several new insights. In general NEWS-DIP-HD estimates are consistent with a previous global analysis of P loading to surface waters (Figure 3; *Harrison et al.*, 2005). However, impressive within-basin spatial heterogeneity is revealed by applying the NEWS-DIP-HD model (Compare Figure 3 A and B). Hot spots for DIP loading tend to occur in urban centers (e.g. in the Northeastern U.S., the United Kingdom, Western Europe, Mexico, Bangladesh, India, Pakistan, China, and Japan). High rates of DIP loading also occur in

humid areas with high predicted rates of P weathering (e.g. in the Brazilian Amazon, W. Africa, Central America, the Northwest U.S., and Indonesia). In addition, inland cells appear to be quite important with respect to their contribution to coastal DIP loading, particularly in the Midwest US, Western Europe, Southern Asia, and Eastern China (Figure 3).

On a half-degree grid-cell basis, predicted DIP yields ranged over several orders of magnitude, from zero in arid zones with little or no population (e.g. Saharan Africa and the Australian interior) to 6,366 kg P km<sup>-2</sup> yr<sup>-1</sup> in the grid cell containing Tokyo, Japan (Figure 3). In general, urban areas are responsible for much of the DIP input to surface waters. In our analysis, the half-degree grid cells containing the world's 19 cities with populations greater than 5 million contribute 0.04 Tg of P to surface waters, or roughly 4% of the global total anthropogenic DIP input. The 214 cities with populations greater than 1 million account for 19% of DIP inputs to surface waters globally, and the 1058 cities with populations greater than 100,000 individuals contribute 35% of global anthropogenic surface water DIP loads. Together, all of the cities with populations greater than 100,000 account for less than 2% of the global land surface, highlighting the intensity of DIP production in urban areas.

In general, areas with high predicted rates of DIP loading to surface waters correspond to areas where P-related water quality problems have been reported (e.g. Midwest US, Western Europe, the United Kingdom, Japan, India, and Eastern China [UNEP 2001; Smith *et al.*, 2003]). However, there are a number of areas globally that have received relatively little attention in terms of focus on eutrophication-related problems, but that are highlighted in this analysis as likely hotspots for DIP loading to

surface freshwaters (e.g. Bangladesh, Southern Brazil, Central Chile, Indonesia, Pakistan, Portions of N. Africa, Eastern Europe and Russia, and Korea).

NEWS-DIP-HD estimates of DIP retention within surface water systems varied widely from cell to cell and from basin to basin. Hotspots for DIP retention are indicated to occur in the St. Lawrence, Volga, Indus, Dneper, Danube, Yangtze, Yellow, Pearl, and Parana, River basins, and in others as well (Figure 4). High rates of DIP retention may also occur in additional river basins, but where information about reservoir locations and sizes and consumptive water use was lacking, zero retention was assumed, making our estimate of DIP retention quite conservative.

### *Sources*

NEWS-DIP-HD predicts that human activity dominated DIP export in half-degree cells accounting for over half (53%) of the Earth's land surface, with a much larger area dominated by DIP point sources than non-point sources (52% versus 1% of the global land surface, respectively). Point source-dominated areas occur throughout both the north and south temperate zones and in much of the populated, arid tropics and subtropics as well. Of the relatively little surface area dominated by non-point sources of DIP, 35% was dominated by manure sources and 65% was dominated by fertilizer sources.

Regions where NEWS-DIP-HD suggests fertilizer P inputs are important as a DIP source include much of New Zealand, portions of Vietnam, Japan, Korea, Finland, Norway, parts of Bangladesh, and isolated half-degree grid cells in the Brazilian Amazon and the Midwest U.S.. Regions where manure P sources are indicated as the single greatest DIP source include Ethiopia, isolated portions of the Brazilian Amazon, China, Nepal, New

Zealand, Madagascar, Venezuela, the Midwest U.S., and southern Canada. There are also a number of regions where the model predicts no DIP input to surface waters (White regions in Figures 3 and 5) due to a lack of P inputs to the landscape. An examination of Figures 3 and 5 together, indicates that many of the high DIP yielding areas are areas where human activities (and most often sewage point sources) dominate DIP inputs to surface waters, though interestingly this is not true in all cases (e.g. the Brazilian Amazon, where NEWS-DIP-HD actually somewhat underestimates DIP transport). Despite the undeniable impact of human activity, and especially P point sources on DIP loading to freshwaters, DIP loading across a significant portion of the earth's land surface is still dominated by non-anthropogenic DIP sources. NEWS-DIP-HD suggests that in 2000 weathering was the dominant source of coastal DIP over 35% of the Earth's land surface (Figure 5). Basins where NEWS-DIP-HD predicts weathering to dominate DIP sources lie across all latitudes, and occur in areas with relatively little human influence and in wet tropical systems such as the Amazon, the Congo, Northern Australia, and Indonesia.

Though a few studies have attempted to attribute sources of TP [Boynton *et al.*, 1995; Baker and Richards, 2002; Moore *et al.*, 2004] and total PO<sub>4</sub> (dissolved plus acid-soluble, but undigested particulate) [Jordan *et al.*, 2003] to river P loading, we were able to locate only one study quantifying the relative importance of different land-based sources specifically to river DIP loading. This one study of a relatively rural portion of the Thames River watershed [Cooper *et al.*, 2002] suggests that point sources account for 77-97% of the river DIP inputs, depending on the year (1995-1999). NEWS-DIP-HD predicts that for the whole Thames River watershed, including the more urban portions,

point sources account for 99% of the DIP loading, a fairly good agreement with the local study.

Comparison of NEWS-DIP predictions with regional studies that estimate sources of other P forms also suggests that NEWS-DIP-HD predictions are reasonable. Studies attributing TP or total PO<sub>4</sub> to point and non-point sources have calculated point source inputs based on data from waste water treatment plants and subtracted that value from total export to calculate contribution from non-point sources. Such studies have estimated that point sources contribute 95% of the TP load the Patuxent River [Boynton *et al.*, 1995] and 50% of the TP load to Baltic rivers [HELCOM 2003]. Assuming TP:DIP ratios of 0.033 and 1 for point and non-point sources respectively (similar to values reported by Cooper *et al.* [2002] for the Thames), this translates to estimated point source contributions of 97 and 67 % for the Patuxent and Baltic, respectively. NEWS-DIP-HD estimates that point sources account for 99 and 92% of the DIP source in the Patuxent and Baltic regions, respectively.

NEWS-DIP-HD suggests that point sources, as opposed to anthropogenic diffuse sources, most often dominate DIP export to coastal regions on global scale. However, in intensively farmed regions, non-point sources of DIP can dominate river and coastal DIP loading. On average DIP export appears to be more often dominated by point sources than river-exported DIN. Whereas global DIN export has been attributed mainly to non-point N sources, particularly N fertilizer [Seitzinger and Kroeze 1998; Caraco and Cole, 2004; Green *et al.*, 2004], global DIP export is influenced mainly by sewage point sources. The dominant role of point sources in controlling DIP export is consistent with previous global analyses [Caraco 1995; Smith *et al.*, 2003; Harrison *et al.*, 2005].

### 3.2.2 Global and Regional Analyses

We estimate that 1.45 Tg P yr<sup>-1</sup> reached river mouths emptying into major ocean basins as DIP in 2000. This estimate is similar to other recent, measurement-based and model-calculated estimates of global DIP export, which range from 0.8 to 2.4 Tg yr<sup>-1</sup> [Pierrou 1976; Meybeck 1982; Richey 1983; Wollast 1983; Smith *et al.*, 2003; Harrison *et al.*, 2005]. Of the 16.49 Tg of P we calculate are loaded on watersheds by human activity globally, we estimate approximately 8.7% is exported by rivers as DIP. Globally, retention of DIP due to reservoir construction and consumptive water use (i.e. excluding P that is assumed to never reach aquatic systems) is conservatively estimated as 0.34 Tg P/yr, roughly 20% of the total DIP delivered annually to the coastal ocean globally and essentially equivalent to the amount of naturally weathered DIP (0.35 Tg P/yr). According to NEWS-DIP-HD, anthropogenic sources account for 76% (1.1 Tg yr<sup>-1</sup>) of the DIP exported to the coastal zone globally, with the remaining 24% (0.35 Tg yr<sup>-1</sup>) attributable to natural weathering processes. This predicted rate of weathering-derived P export is virtually identical to the rate predicted by Meybeck [1982] (0.4 Tg yr<sup>-1</sup>), an estimate based on a study of relatively unimpacted rivers.

According to NEWS-DIP, P point sources alone account for over half (72%) of the total global DIP export via rivers. Inorganic fertilizer (2.0%) and animal manure (2.0%) contribute substantially smaller fractions of the coastal DIP load. On every continent and in every ocean basin, human sewage is the largest source of anthropogenically-derived exported DIP, followed by P from P-based detergents. According to NEWS-DIP predictions, Asia is the largest continental exporter of DIP

(Figure 6), contributing 38% ( $0.72 \text{ Tg yr}^{-1}$ ) of the total global DIP export from watersheds to the global coastal ocean and inland seas. Export rates for other continents vary substantially, with Europe, S. America, N. America (including Greenland), Africa, Oceania (including New Zealand), and Australia each exporting 0.27, 0.32, 0.26, 0.21, 0.11,  $0.02 \text{ Tg of DIP P yr}^{-1}$ , respectively. Of the world's ocean basins, NEWS-DIP predicts that the Atlantic Ocean receives the most DIP from land-based sources ( $0.59 \text{ Tg yr}^{-1}$ ), followed by the Pacific and Indian oceans (0.50 and 0.25, respectively), the Mediterranean Sea ( $0.08 \text{ Tg yr}^{-1}$ ), and the Arctic Ocean ( $0.03 \text{ Tg yr}^{-1}$ ).

Continental and ocean basin calculations suggest that humans have equaled or outstripped natural processes as a source of DIP to the coast on all continents (ranging from 57% of DIP inputs in S. America to 92% of DIP inputs in Europe) and all ocean basins except for the arctic, where anthropogenically derived P accounts for 48% of P sources (Figure 6). Although it is difficult to compare 1995 and 2000 predictions due to changes in methods and the DIP model between the previous model run which, for example, did not include P-based detergents [*Harrison et al.*, 2005] and this model run which does include such detergents, such a comparison suggests that human influence on DIP export increased substantially between 1995 and 2000. The greatest increases between 1995 and 2000 were observed in Asia and the Pacific Ocean.

### **3.3 Sources of Uncertainty and Future Directions**

The NEWS-DIP-HD model represents a significant step forward in terms of capacity to model river DIP export at the global scale. However, there is still significant room for model improvement. As global datasets improve, there will be opportunities to

greatly improve estimates of river DIP export. In the following two sections, we use patterns of model error along with model efficiency and sensitivity analyses (Tables 3 and 4) to infer where improvements to global datasets and model improvements are likely to be most useful in enhancing DIP yield estimates. We also examine the potential implications of assumptions made during the model development process, and suggest future directions in the field of global nutrient modeling.

### ***3.3.1 Model Efficiency and Sensitivity***

An analysis of model efficiency, wherein model components were removed sequentially to evaluate the contribution of each to model predictive capacity, suggests weathering and sewage point source sub-models are particularly important model drivers (Table 3). This analysis suggests that consumptive water use and P retention in reservoirs also play significant roles in the correct determination of DIP yield by NEWS-DIP-HD, but that anthropogenic non-point sources, while important in certain regions, are less vital in explaining DIP yield than other model components at the global scale (Table 3). Removal of the detergent point source term from NEWS-DIP-HD actually improved model efficiency slightly.

A sensitivity analysis of NEWS-DIP-HD in which model inputs and coefficients were increased by 10% in order to evaluate model response (Table 5) suggests that the NEWS-DIP-HD model is fairly robust. Ten percent changes in all input parameters, coefficients, and all possible combinations of coefficients result in average changes in predicted DIP yield of 10% or less, and in most cases substantially less. Of course sensitivities of individual half-degree pixels vary substantially more, depending on the

dominant control on DIP transport in a given region. As with the original NEWS-DIP model, NEWS-DIP-HD predictions are somewhat sensitive to small changes in the weathering-related parameters  $W_{max}$ ,  $R$ ,  $a$  and  $b$  (Table 5). NEWS-DIP-HD's sensitivity to changes in the weathering submodel coefficients suggests that any improvement in NEWS-DIP-HD's representation of weathering-derived P is likely to improve model predictive capacity. Finally, NEWS-DIP output is relatively insensitive to removal of its non-point P source term (Table 3) and to manipulation of non-point source input datasets (Table 4). This suggests that inaccuracies in fertilizer and manure input datasets have relatively minor impacts on regional and global model predictions, especially in comparison with inaccuracies associated with other model inputs. However the importance of these terms is likely to vary spatially.

### ***3.2.2. Future Directions***

Taken together, model efficiency and sensitivity analyses suggest several areas for future improvements in NEWS-DIP-HD. For example, these analyses both suggest that point-sources are important in driving predictions of DIP export (Tables 3 and 4). These analyses also suggest that NEWS-DIP predictions are sensitive to estimates of weathering (Tables 3 and 4). In future DIP export models, it may be possible to reduce uncertainty in estimates of weathering rates by refining the NEWS-DIP-HD sub-model for predicting weathering-derived P (eq. 4) through the inclusion of factors thought to influence weathering rates such as temperature, soil type, soil parent material, and pH as improved global datasets become available. Finally, efficiency analysis suggests that our characterization of the linkages between human activity, P-based detergent use, and DIP

loading of surface waters could bear some improvement.

NEWS-DIP-HD somewhat underestimates DIP export and yield from Amazon sub-basins for both the Amazon main stem and its tributaries (mean underestimate 43%; Figure 2a and 2b). In addition, there is still a significant amount of unexplained variation. However, in general, NEWS-DIP-HD performs as well as the original NEWS-DIP model. The strong performance of NEWS-DIP-HD is encouraging but also curious given that NEWS-DIP-HD was not re-calibrated and there is no explicit in-stream loss pathway for DIP in the NEWS-DIP-HD aside from loss in reservoirs and loss due to consumptive water use. It may be that the half-degree resolution utilized by NEWS-DIP-HD is still coarse enough so that small-scale variation in DIP yield due to in-stream processing of P is averaged out. It may also be that DIP acts relatively conservatively because it is in dynamic equilibrium with particulate P in freshwater aquatic systems (As described in *Froelich et al.* [1988]).

In future global DIP export models it will be important to improve representation of reservoir retention. Including DIP sinks other than reservoirs and consumptive water use may also improve the model. For example, natural lakes, river-associated wetlands, and floodplains may account for significant levels of DIP retention, but are not treated explicitly by the NEWS-DIP-HD model. In addition, retention on land may also constitute an important DIP sink as re-use of sewage as fertilizer (night soil), conservation tillage practices, and highly weathered, P-deficient soils, and P-limited terrestrial (or aquatic) ecosystems all may lead to DIP retention within watersheds. At present, terrestrial sinks for DIP are represented in the model as sewage treatment, weathering efficiency, and fertilizer and manure transfer efficiency terms. This rather

simple treatment of terrestrial P sinks results from a lack of more detailed global scale input data, and it is possible that future inclusion of such data may improve the NEWS-DIP-HD model significantly. Though our analysis is currently limited to large (>5<sup>th</sup> order) rivers, this problem will most likely be solved incrementally as increasingly reliable, finer resolution spatial datasets of model-drivers become available.

With improved resolution and quality of input and validation datasets and faster computers it will become possible to improve the spatial resolution of DIP export models even further so that it will be possible to examine P dynamics in even smaller river systems than has been possible in this analysis. The generation of improved input and validation data will likely lead to more accurate model predictions and additional insights. Higher resolution validation data will facilitate the enhanced representation of DIP retention as well as the inclusion of interactions between elements and elemental forms. Also, as improved temporal resolution datasets of runoff and land-use become available, it should be possible to use NEWS-DIP-HD to examine sub-annual patterns of DIP export. Incorporating such sub-basin spatial and sub-annual temporal variability into global DIP export modeling efforts will constitute significant advances in understanding of the global P cycle and effects. It should also be possible to use the insights and approaches developed in the analysis associated with this effort to further enhance NEWS models that predict the transport of other biogeochemically relevant elements (e.g. N, silica, and carbon) and forms (e.g. dissolved, particulate, organic, and inorganic forms) of these elements. For the present, however, NEWS-DIP-HD represents a significant advancement in its own right as the first spatially explicit, global DIP export model with the capacity to route DIP downstream through watersheds, thereby maintaining within-

basin spatial variability in P loading and P sinks.

#### **4. Acknowledgments**

We are grateful to UNESCO-IOC, NASA, USGS, and CALFED for supporting this work and to Charlie Vörösmarty, Balazs Fekete, Wil Wollheim and the rest of the Global NEWS working group for useful discussion and feedback. This work was supported by grants to J. A. Harrison from California Sea Grant (award number RSF8), from the US Geological Survey 104b program, and from the NASA-IDS program (award number 06-IDS06-009). However, any opinions, findings, and conclusions or recommendations expressed in this material are those of the authors and do not necessarily reflect the views of NASA, USGS, CALFED, or other funding agencies.

## 5. References Cited

Alexander, R. B., J. R. Slack, A. S. Ludtke, K. K. Fitzgerald, and T. L. Schertz. Data from selected U.S. Geological Survey national stream water quality monitoring networks (WQN). U.S.G.S. Digital Data Series DDS-37. U. S. Geological Survey. 1996.

Alexander, R. B., R. A. Smith, G. E. Schwarz, E. W. Boyer, J. V. Nolan, and J. W. Brakebill. Differences in phosphorus and nitrogen delivery to the gulf of Mexico from the Mississippi river basin, *Environmental Science and Technology* 42(3), 822-830, 2008.

Baker, D. B., and R. P. Richards. Phosphorus budgets and riverine phosphorus export in northwestern Ohio watersheds. *Journal of Environmental Quality* 31 (1), 96-108, 2002.

Baffaut, C., and V. W. Benson. Modeling flow and pollutant transport in a karst watershed with SWAT, *Transactions of the ASABE*, 52(2), 469-479, 2009.

Bennett, E. M., S. R. Carpenter, and N. F. Caraco. Human impact on erodable phosphorus and eutrophication: A global perspective. *Bioscience* 51 (3), 227-234, 2001.

Bouwman, A.F., G.v. Drecht, J.M. Knoop, A.H.W. Beusen, and C.R. Meinardi, Exploring changes in river nitrogen export to the world's oceans, *Global Biogeochemical Cycles*, 19 (1), GB1002. 2005

Boynton, W. R., J. H. Garber, R. Summers, and W. M. Kemp. Inputs, Transformations, and transport of nitrogen and phosphorus in Chesapeake Bay and selected tributaries. *Estuaries* 18 (1B):285-314, 1995.

Bradford, M. E. and H. R. Peters, The relationship between chemically analyzed phosphorus fractions and bioavailable phosphorus, *Limnology and Oceanography*, 32, 1124-1137, 1987.

Caraco, N. F., and J. J. Cole. Human impact on nitrate export: an analysis using major world rivers. *Ambio* 28(2),167-170, 1999.

Caraco, N. F., Influence of human populations on P transfers to aquatic systems: a regional scale study using large rivers, in *Phosphorus in the Global Environment: Transfers, Cycles and Management (SCOPE 54)*, edited by H. Tiessen, pp. 236-244, Wiley, New York, 1995.

Conley, D.J., H.W. Paerl, R.W. Howarth, D.F. Boesch, S.P. Seitzinger, K.E. Havens, C. Lancelot, and G.E. Likens. 2009. Controlling Eutrophication: Nitrogen and Phosphorus. *Science* 20(5917): 1014-1015, DOI: 10.1126/science.1167755.

Cooper, D. M., W. A. House, L. May, and B. Gannon. The phosphorous budget of the Thame catchment, Oxfordshire, UK: 1.Mass Balance. *The Science of the Total Environment* 282-283:233-251, 2002.

Devol, A., B. Forsberg, J. Richey, and T. Pimentel (1995), Seasonal Variation in Chemical Distributions in the Amazon (Solimões) River: A Multiyear Time Series, *Global Biogeochem. Cycles*, 9(3), 307-328.

Diaz, R.J., and R. Rosenberg. 2008. Spreading dead zones and consequences for marine ecosystems, *Science*, 321, 5891, 926-929.

Ekholm, P., Bioavailability of phosphorus in agriculturally loaded rivers in southern Finland, *Hydrobiologia*, 287, 179-194, 1994.

FAO (2008), FAOSTAT database collections ([www.apps.fao.org](http://www.apps.fao.org)), Food and Agriculture Organization of the United Nations, Rome.

Fekete, B. M., Vörösmarty, C. J. and Grabs, W. 2002. High-resolution fields of global runoff combining observed river discharge and simulated water balances. *Global Biogeochemical Cycles* 16: 1042, doi:10.1029/1999GB001254.

Fisher T.R., Gustafson A.B., K. Sellner, R. Lacouture, L. W. Haas, R. L. Wetzel, R. Magnien, D. Everitt, B. Michaels, and R. Karrh. Spatial and temporal variation of resource limitation in Chesapeake Bay. *Marine Biology* 133 (4), 763-778, 1999.

Fixen, P.E., and West, F. B. Nitrogen fertilizers: meeting contemporary challenges. *Ambio* 31(2), 169-176, 2002.

Fox, L. E., A model for inorganic control of phosphate concentrations in river waters, *Geochimica et Cosmochimica Acta*, 53, 417-428, 1989.

Froelich, P. N. 1988. Kinetic control of dissolved phosphate in natural rivers and estuaries: A primer on the phosphate buffer mechanism. *Limnol. Oceanogr.* 33, 649-668.

United Nations Global Environmental Monitoring System (GEMS)  
(<http://www.gemswater.org/index.html>).

Green, P. A., C. J. Vörösmarty, M. Meybeck, J. N. Galloway, B. J. Peterson, and E. W. Boyer. Pre-industrial and contemporary fluxes of nitrogen through rivers: a global assessment based on typology. *Biogeochemistry* 68, 71-105, 2004.

Harrison, P. J., M. H. Hu, Y. P. Yang, and X. Lu, Phosphate limitation in estuarine and coastal waters of China, *Journal of Experimental Marine Biology and Ecology*, 140, 79-87, 1990.

Harrison, J.A., S.P. Seitzinger, A.F. Bouwman, N.F. Caraco, A.H.W. Beusen and C. Vörösmarty (2005a) Dissolved inorganic phosphorus export to the coastal zone: results from a spatially explicit, global model (NEWS-DIP), *Global Biogeochemical Cycles*, **19**, GB4S03, doi:10.1029/2004GB002357, 1-15.

International Commission on Large Dams (ICOLD). 2003. World Register of Dams. Paris, France: International Commission on Large Dams.

HELCOM. Executive Summary of the Fourth Baltic Sea Pollution Load Compilation (PLC-4), Helsinki Commission Baltic Marine Environment Protection Commission, 2003.

Howarth, R. W., G. Billen, D. Swaney, A. Townsend, N. Jaworski, K. Lajtha, J. A. Downing, r. Elmgren, N. Caraco, T. Jordan, F. Berendse, J. Freney, V. Kudeyarov, P.

Murdoch, and Z. L. Zhu. Regional nitrogen budgets and riverine N&P fluxes for the drainages to the North Atlantic Ocean: natural and human influences. *Biogeochemistry* 35:75-139, 1996.

Jensen, H. S., K. J. McGlathery, R. Marino, and R. W. Howarth, Forms and availability of sediment phosphorus in carbonate sand of Bermuda seagrass beds, *Limnology and Oceanography*, 43, 799-810, 1998.

Jordan, T. E., D. E. Weller, and D. L. Correll. Sources of nutrient inputs to the Patuxent River Estuary. *Estuaries* 26 (2A):226-243, 2003.

Mackenzie, F.T., Ver, L.M., and Lerman, A. 1998. Coupled biogeochemical cycles of carbon, nitrogen, phosphorous and sulfur in the land-ocean-atmosphere system, p.42-100. *In: J.N. Galloway and J.M. Melillo [eds.]. Asian change in the context of global climate change.* Cambridge University Press.

Melack, J. M., Transport and transformations of P, fluvial and lacustrine ecosystems, in *Phosphorus in the global environment*, edited by H. Tiessen, pp. 245-254, John Wiley & Sons, New York, 1995.

Meybeck, M., Carbon, nitrogen, and phosphorus transport by world rivers, *American Journal of Science*, 282, 401-450, 1982.

Meybeck, M. and A. Ragu. River discharges to the oceans: an assessment of suspended solids, major ions, and nutrients. Environment and Assessment. Paris: United Nations Environment Programme. 1-245, 1996.

Moore, R.B., C.M. Johnston, K.W. Robinson, and J.R. Deacon, Estimation of total nitrogen and phosphorus in New England Streams using spatially referenced regression models, U.S. Geological Survey Scientific Investigations Report 2004-5012, Pembroke, New Hampshire, pp. 1-41, 2004.

Murrell, M. C., R. S. Stanley, E. M. Lores, G. T. DiDonato, L. M. Smith, and D. A. Flemer, Evidence that phosphorus limits phytoplankton growth in a Gulf of Mexico estuary: Pensacola Bay, Florida, USA, *Bulletin of Marine Science*, 70, 155-167, 2002.

Nash, J. E. and J. V. Sutcliffe. River flow forecasting through conceptual models: Part 1 - A discussion of principles. *Journal of Hydrology* 10 (1970):282-290, 1970.

Pierrou, U. The global phosphorus cycle. In: *Nitrogen, phosphorus, and sulfur - Global Cycles*, edited by B. H. Svensson and R. Soderlund, Stockholm:SCOPE, 1976, p. 75-88.

Richey, J. E.. The Phosphorus Cycle. In: *The major biogeochemical cycles and their interactions*, edited by E. T. Degens, S. Kempe, and J. E. Richey, New York:John Wiley and Sons, 1983, p. 51-56.

Seitzinger, S. P. and C. Kroeze. Global distribution of nitrous oxide production and N inputs in freshwater and coastal marine ecosystems. *Global Biogeochemical Cycles* ; 12 (1):93-113, 1998.

Smith, S. V., D. P. Swaney, L. Talaue-Mcmanus, J. D. Bartley, P. T. Sandhei, C. J. McLaughlin, V. C. Dupra, C. J. Crossland, R. W. Buddemeier, B. A. Maxwell, and F. Wulff. Humans, hydrology, and the distribution of inorganic nutrient loading to the ocean. *Bioscience* 53 (3), 235-245, 2003.

Sylvan JB, Dortch Q, Nelson DM, Brown AFM, Morrison W, Ammerman JW. 2005. Phosphorus limits phytoplankton growth on the Louisiana shelf during the period of hypoxia formation. *Environmental Science and Technology*, 40(24), 7548-7553

Thieu, V., G. Billen, and J. Garnier. Nutrient transfer in three contrasting NW European watersheds: The Seine, Somme, and Scheldt Rivers. A comparative application of the Seneque/Riverstrahler model, *Water Research*, 43(6), 1740-1754.

United Nations Environment Programme (UNEP) - Global Environment Monitoring System (GEMS) Water Programme, 2001; National Water Research Institute Environment Canada, Ontario, 2001.

<http://www.unep.org/dewa/assessments/ecosystems/water/vitalwater/10.htm>

Van Dreht, G., A.F. Bouwman, J.A. Harrison, and J. Knoop (In Press) Global nitrogen

and phosphate in urban waste water for the period 1970-2050, *Global Biogeochemical Cycles*.

Ver, L. M., F. T. MacKenzie, and A. Lerman. Biogeochemical responses of the carbon cycle to natural and human perturbations: past, present, and future. *American Journal of Science*, 299 (Sept./Oct./Nov.):762-801, 1999.

Vörösmarty, C.J., B.M. Fekete, M. Meybeck, and R. Lammers. 2000a. A simulated topological network representing the global system of rivers at 30-minute spatial resolution (STN-30). *Global Biogeochemical Cycles*, 14:2 599-621.

Vörösmarty, C. J., B. M. Fekete, M. Meybeck, and R. B. Lammers. 2000b. Geomorphometric attributes of the global system of rivers at 30-minute spatial resolution. *Journal of Hydrology*, 237 (2000):17-39.

Weller, D. E., T. E. Jordan, and D. L. a. L. Z. J. Correll, Effects of land-use change on nutrient discharges from the Patuxent River watershed, *Estuaries*, 26, 244-266, 2003.

Wollast, R.. Interactions in estuaries and coastal waters. In: *The major biogeochemical cycles and their interactions*, edited by B. Bolin and R. B. Cook, New York:John Wiley and Sons, 1983, p. 385-410.

## Table Legends

**Table 1.** Input datasets for NEWS-DIP-HD

**Table 2.** Metrics of model performance for NEWS-DIP-HD and other models, validated with dataset described in section 2.2 unless otherwise noted.  $R^2$  is model efficiency as defined in section 3.1, and  $r^2$  is the coefficient of determination. Errors are computed as the difference between the predicted and measured values of stream phosphorus yield ( $\text{kg km}^{-2} \text{ yr}^{-1}$ ) expressed as a percentage of the measured export (section 3.1).

**Table 3.** Model efficiencies for comparison of log-transformed measured and model-predicted DIP yield, using NEWS-DIP-HD with various components removed. All available measurement data were used for this analysis.

**Table 4:** Results of a sensitivity analysis indicating mean change in predicted DIP yield as a function of increasing input datasets and model parameters by +10%.

## Figure Legends

**Figure 1.** Spatial distribution of basins used to validate the NEWS-DIP-0.5 model ( $n=206$  overall). Xs represent sampling stations within the Amazon River Basin (Devol et al., 1995). Plus signs represent sampling stations monitored by the Global Environment Monitoring System (GEMS) Water program not used in Harrison et al., 2005 ( $n= 33$ ; <http://www.gemswater.org/index.html>). Hollow circles represent sampling stations within the Mississippi, Sacramento, and San Joaquin River Basins ( $n=54$ ; Data source: Alexander et al. (1996)). Black diamonds represent stations used in calibration and validation of the original NEWS-DIP model ( $n = 118$ ; Harrison et al., 2005). See Appendix B for data, model output, and station names.

**Figure 2.** Measured versus modeled DIP load (Top;  $\text{kg P basin}^{-1} \text{ yr}^{-1}$ ) and yield (Bottom;  $\text{kg P km}^{-2} \text{ yr}^{-1}$ ) for Mississippi River Basin stations (hollow circles), global coastal stations included in Harrison et al. (2005; black diamonds), global stations from

the United Nations Global Environmental Monitoring System (GEMS; plus signs), and data from the Amazon Basin ([*Devol et al.*, 1995]; exes). See Appendix B for data, model output, and basin names. The 1:1 line is also shown. Symbols are the same as in Figure 1.

**Figure 3.** A) NEWS-DIP-predicted DIP yield by half-degree grid cell ( $\text{kg P km}^{-2} \text{ yr}^{-1}$ ) and B) NEWS-DIP-HD-predicted DIP yield by half-degree grid cell ( $\text{kg P km}^{-2} \text{ yr}^{-1}$ ). White areas are either endoreic (A) or have a predicted DIP loading to surface waters equal to zero (B).

**Figure 4.** NEWS-DIP-HD-estimated DIP retention ( $\text{kg P km}^{-2} \text{ yr}^{-1}$ ) globally by half degree. Estimates without information regarding reservoir locations and consumptive water use were assumed to retain no DIP, making this quite a conservative estimate of DIP retention within watersheds globally.

**Figure 5.** Dominant source of DIP by half-degree grid cell. “Dominant source” is defined as the modeled source that NEWS-DIP-HD predicts contributes the largest single fraction of DIP to the coast.

**Figure 6.** River export of DIP ( $\text{Tg P yr}^{-1}$ ) from continents and to ocean basins. Relative influence of various P sources calculated according to NEWS-DIP-HD.

**Table 1.** Input datasets for NEWS-DIP-HD

Dataset	Resolution	Year	Source(s)
Basin Delineations	0.5°	1960-1994	STN30 [Vörösmarty et al., 2000a and 2000b]
River Networks	0.5°	1960-1994	STN30 [Vörösmarty et al., 2000a and 2000b]
Water Runoff and Discharge	0.5°	1960-1994	Fekete et al., 2002
Population Density	0.5°	2000	Bouwman et al., 2004
Fertilizer P Inputs	0.5°	2000	Bouwman et al., Submitted
Manure P Inputs	0.5°	2000	Bouwman et al., Submitted
Crop Harvest P Export	0.5°	2000	Bouwman et al., Submitted
Sewage P Inputs	0.5°	2000	Bouwman et al., 2004
Detergent P Inputs	0.5°	2000	Van Drecht et al., In Press
Dam Locations and Volumes	0.5°	2000	ICOLD 2003

**Table 2.** Metrics of model performance for NEWS-DIP-HD and other models, validated with dataset described in section 2.2 unless otherwise noted.  $R^2$  is model efficiency as defined in section 3.1, and  $r^2$  is the coefficient of determination. Errors are computed as the difference between the predicted and measured values of stream phosphorus yield ( $\text{kg km}^{-2} \text{yr}^{-1}$ ) expressed as a percentage of the measured export (section 3.1).

Model	DIP yield ( $\text{kg P km}^{-2} \text{yr}^{-1}$ )		DIP load (Ton P basin $^{-1}$ )		IQR <sup>a</sup>	Prediction Errors (%)			
	$r^2$	$R^2$	$r^2$	$R^2$		min.	25 <sup>th</sup>	75 <sup>th</sup>	max.
NEWS-DIP <sup>b</sup>	0.56	0.51	0.60	0.47	247	-90	-9	239	2542
NEWS-DIP-HD <sup>c</sup>	0.60	0.51	0.78	0.77	82	-90	-50	32	4811
NEWS-DIP-HD <sup>d</sup>	0.45	0.29	0.52	0.52	221	-99.6	-46	175	4574
NEWS-DIP-HD <sup>e</sup>	0.50	0.39	0.62	0.61	204	-99.6	-47	157	4811
LOICZ-DIP <sup>f</sup>	0.46	0.17	0.52	0.46	502	-78	-16	487	13672
CARACO <sup>g</sup>	0.41	0.34	0.54	0.43	692	-96	30	722	19982

<sup>a</sup> Interquartile range (difference between the 25<sup>th</sup> and 75<sup>th</sup> percentiles of the distribution of errors).

<sup>b</sup> Harrison et al. [2005] model using validation basins only

<sup>c</sup> NEWS-DIP-HD with USGS-WQN data

<sup>d</sup> NEWS-DIP-HD with data from Harrison et al. [2005]

<sup>e</sup> NEWS-DIP-HD using all validation data

<sup>f</sup> Smith et al. [2003] model using validation data from Harrison et al. [2005]

<sup>g</sup> Caraco et al. [1996] model using validation data from Harrison et al. [2005]

**Table 3.** Model efficiencies for comparison of log-transformed measured and model-predicted DIP yield, using NEWS-DIP-HD with various components removed. All available measurement data were used for this analysis.

Treatment	Model efficiency ( $R^2$ ) DIP Yield ( $\text{kg km}^{-2} \text{yr}^{-1}$ )	%Change in model efficiency resulting from component removal DIP Yield
Complete Model	0.41	
No Weathering P	-1.32	-422
No Fecal Point Sources	-0.39	-195
No Consumptive Water Use	0.23	-44
No Reservoir Retention	0.32	-22
No Non-point Sources	0.41	0
No Detergent Point Sources	0.44	7

**Table 4:** Results of a sensitivity analysis indicating mean change in predicted DIP yield as a function of increasing input datasets and model parameters by +10%.

Treatment	Parameter or input	Mean change in predicted DIP ( $\text{kg km}^{-2} \text{yr}^{-1}$ ) (%)
+ 10%	Sewage P	5.45
+ 10%	Runoff (m)	3.43
+ 10%	$W_{max}$	3.30
+ 10%	Detergent P	0.98
+ 10%	Manure P	0.38
+ 10%	Lmax	0.27
+ 10%	Fertilizer P	0.24
+ 10%	P Removal by Crop Export and Animal Grazing	-0.35
+ 10%	$b$	-1.03
+ 10%	% Retention in Reservoirs	-1.717
+ 10%	$a$	-2.96
+ 10%	Consumptive Water Use	-10.0

## Appendix A. Variable definitions for NEWS-DIP model

Variable	Definition
$DIP$	DIP yield ( $\text{kg P km}^{-2} \text{ yr}^{-1}$ )
$Q_{act}$	Measured discharge after dam construction ( $\text{km}^3 \text{ H}_2\text{O yr}^{-1}$ )
$Q_{nat}$	Measured discharge prior to dam construction ( $\text{km}^3 \text{ H}_2\text{O yr}^{-1}$ )
$D$	Fraction DIP retained in reservoirs (0-1)
$R$	Runoff ( $\text{m H}_2\text{O yr}^{-1}$ )
$H$	Human population density (individuals $\text{km}^{-2}$ )
$P_{sw}$	Per capita DIP yield ( $\text{kg P individual}^{-1} \text{ yr}^{-1}$ )
$a$	Unit-less coefficient defining how non-point DIP and weathered DIP respond to runoff; for NEWS-DIP set equal to 0.85
$b$	Unit-less coefficient defining how non-point DIP and weathered DIP respond to runoff; for NEWS-DIP set equal to 2
$W_{max}$	Maximum DIP yield due to weathering alone ( $\text{kg P km}^{-2} \text{ yr}^{-1}$ ); for NEWS-DIP set equal to 26
$L_{max}$	Maximum fraction of applied manure and fertilizer P lost to coastal zone as DIP; for NEWS-DIP set equal to 0.04
$P_{fert}$	P applied to watersheds as inorganic fertilizer ( $\text{kg P km}^{-2} \text{ yr}^{-1}$ )
$P_{am}$	P applied to watersheds as manure ( $\text{kg P km}^{-2} \text{ yr}^{-1}$ )
$P_{sew}$	DIP entering surface water from sewage ( $\text{kg P km}^{-2} \text{ yr}^{-1}$ )
$P_{det}$	DIP entering surface water from P-based detergents ( $\text{kg P km}^{-2} \text{ yr}^{-1}$ )
$DIP_{Weathering}$	DIP entering surface water from non-anthropogenic weathering of minerals ( $\text{kg P km}^{-2} \text{ yr}^{-1}$ )
$DIP_{Fertilizer}$	DIP entering surface water from P-based fertilizers ( $\text{kg P km}^{-2} \text{ yr}^{-1}$ )
$DIP_{Manure}$	DIP entering surface water as a result of manure production or application ( $\text{kg P km}^{-2} \text{ yr}^{-1}$ )

**Appendix B.** Data used for model evaluation

River	Latitude <sup>a</sup>	Longitude <sup>a</sup>	Upstream Basin Area (km <sup>2</sup> )	Median Discharge (km <sup>3</sup> /yr)	Median DIP (mg P/L)	Source <sup>a</sup>
Alabama	30.5	-88	114788.8	69.35	0.010	4
Altamaha	31.6544	-81.8281	36260.0	11.25	0.026	4
Amazon	0.1	-49	6112000.0	6590.00	0.020	4
Amguema	68.1	-177.4	29600.0	9.20	0.012	4
Amur	53.1	140.44	1855000.0	344.00	0.021	4
Anabar	72	114.1	79000.0	13.30	0.001	4
Apalachicola	29.67	-84.97	51451.3	29.20	0.006	4
Arkansas	35.25	-94.25	389914.9	37.74	0.038	3
Arkansas	34.75	-92.25	409964.0	49.54	0.034	3
Arkansas	37.25	-97.25	113216.1	1.67	0.414	3
Arkansas	38.25	-102.25	65811.6	0.26	0.024	3
Arkansas	34.25	-91.75	415628.3	75.78	0.031	3
Arkansas	38.25	-105.25	10422.1	0.88	0.029	3
Arkansas	36.75	-96.75	141063.7	7.48	0.074	3
Arkansas	36.25	-96.25	193252.0	8.04	0.088	3
Balsas	17.55	-102.1	112000.0	14.00	0.095	4
Barito	-3.32	114.29	66000.0	86.80	0.005	4
Bei Jiang	23.25	112.25	343513.0	111.35	0.004	2
Bug	47.33	30.47	63700.0	3.40	0.097	4
Cauweri	10.45	79.5	88000.0	20.90	0.100	4
Chao Phrya	13.44	100.3	111435.0	27.80	0.026	4
Chiang Jiang	32.06	121.04	1808000.0	928.00	0.020	4
Churchill (Hud.)	58.47	-94.12	298000.0	25.83	0.006	4
Colorado	32.75	-114.75	794444.0	22.30	0.103	2
Colorado (Ari)	32.44	-114.38	639000.0	0.10	0.102	4
Columbia	46.12	-123.5	669000.0	236.00	0.015	4
Connecticut	41.9872	-72.6058	25019.4	15.74	0.020	4
Dalalven	60.38	17.27	25000.0	9.84	0.002	4
Danube	47.25	20.25	70222.6	14.91	0.087	2
Danube	47.75	19.25	182903.0	73.70	0.195	2
Danube			805000.0	201.25	0.183	4
Daugava	56.53	24.08	87900.0	20.40	0.037	4
Dnepr	46.3	32.18	504000.0	53.40	0.036	4
Dnestr	46.1	30.19	72100.0	10.70	0.056	4
Don	47.25	40.25	391664.0	30.33	0.133	2
Don	47.15	39.45	422000.0	20.70	0.042	4
Drammenselva	59.44	10.15	17000.0	8.10	0.002	4
Eastmain	52.15	-78.05	46400.0	28.20	0.022	4
Ebro	42.25	-2.25	11386.4	2.51	0.137	2
Ebro	40.82	0.52	84000.0	9.24	0.115	4
Elbe	53.5	9	146000.0	23.70	0.390	4
Evros	40.88	26.17	55000.0	6.80	0.280	4
Fraser	49.23	-121.27	220000.0	112.00	0.050	4
Fuchun Jiang	30.18	120.07	54349.0	37.30	0.046	4
Gambia	13.31	-14.5	42000.0	4.90	0.015	4

Ganges	24.05	89.02	1050000.0	493.00	0.075	4
Ganges- Brahmaputra- Meghna	23.75	89.25	952679.0	170.16	1.036	2
Ganges- Brahmaputra- Meghna	25.25	89.75	548939.0	401.31	1.072	2
Ganges- Brahmaputra- Meghna	24.25	90.75	59040.8	104.02	0.743	2
Garonne	44.25	0.14	55000.0	17.20	0.104	4
Glama	59.36	11.07	41200.0	19.90	0.008	4
Grijalva	17.75	-92.75	5896.4	6.00	0.108	2
Grijalva	18.36	-92.39	36400.0	23.00	0.085	4
Guadiana	38.75	-6.75	40779.5	2.32	0.263	2
Guadiana	37.13	-7.24	72000.0	9.00	0.057	4
Hunter	-32.9	151.8	21411.4	0.47	0.062	4
Huang He	37.44	118.36	752000.0	41.00	0.020	4
Hudson			34700.0	17.70	0.060	4
Illinois	41.25	-88.75	21390.7	7.83	0.278	3
Illinois	39.75	-90.75	69264.0	27.79	0.132	3
Indigirka	69.6	147.5	305000.0	50.40	0.005	4
Indus	31.25	73.75	34028.9	1.07	0.422	2
Indus	25.23	68.24	916000.0	57.00	0.520	4
Kamchatka	56.14	162.28	55900.0	33.10	0.075	4
Khatanga	72.55	106	364000.0	85.30	0.006	4
Klamath	41.5144	-123.9992	31339.0	14.55	0.018	4
Kolyma	68.7	158.7	526000.0	70.80	0.006	4
Kuban	45.16	37.24	57900.0	13.40	0.030	4
Kymjoki	60.3	26.52	37200.0	9.68	0.010	4
La Plata	-25.75	-54.75	931200.0	400.39	0.031	2
La Plata	-27.75	-58.75	2177480.0	557.85	0.032	2
La Plata	-26.75	-58.25	994251.0	120.42	0.037	2
La Plata	-32.75	-60.75	2612380.0	589.28	0.052	2
La Plata	-34.25	-58.25	3019553.0	765.69	0.032	2
La Plata	-32.25	-58.25	264486.0	143.03	0.045	2
La Plata	-31.25	-57.75	243471.0	138.15	0.014	2
La Plata	-30.25	-57.75	219576.0	131.15	0.007	2
Lena	70.7	127.4	2430000.0	532.50	0.004	4
Liao	40.5	121.48	219000.0	16.20	0.053	4
Loire	47.16	-2.11	112000.0	26.00	0.090	4
Luan	39.2	119.1	54000.0	4.20	0.012	4
MacKensie	68.16	-133.4	1787000.0	308.00	0.004	4
Magdalena	11.06	-74.51	235000.0	237.00	0.120	4
Mahanadi	30.3	86.75	52094.4	50.61	0.038	4
Manacapuru	-3.25	-60.75	2235312.0	3195.35	0.022	1
Mekong	11.25	105.25	746412.0	398.60	0.022	2
Meuse	51.49	5.01	29000.0	10.20	0.230	4
Mezen	65	45.6	56000.0	20.40	0.023	4
Mino	42.25	-7.75	11404.7	5.76	0.019	2
Mississippi	29.9508	-90.1381	2916081.0	527.95	0.084	4

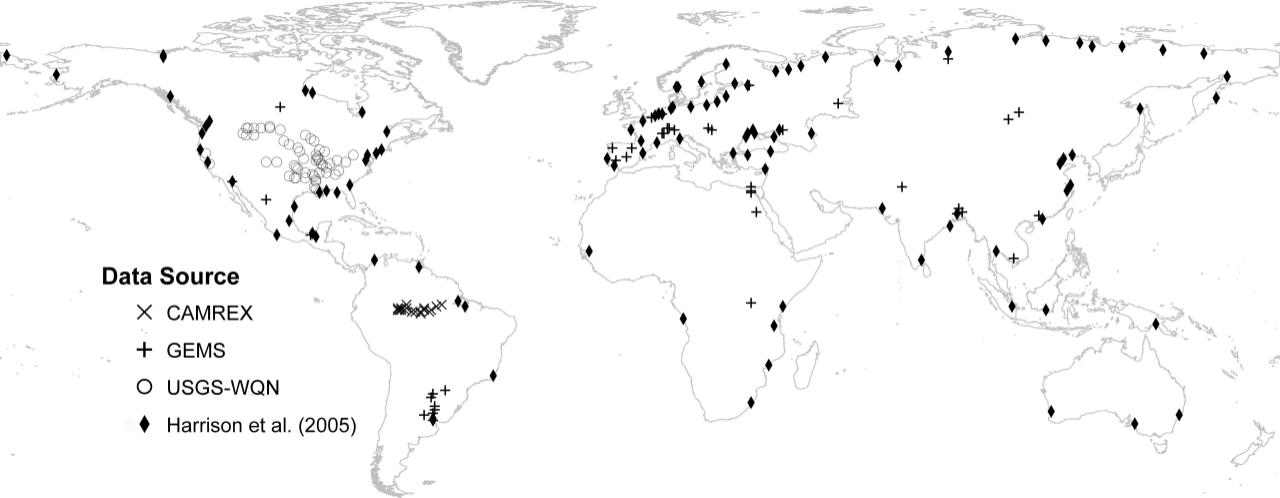
Mississippi	33.25	-91.25	2928240.4	664.84	0.070	3
Mississippi	29.75	-90.25	2926505.1	527.97	0.086	3
Mississippi	41.75	-90.25	221703.0	68.84	0.063	3
Mississippi	40.25	-91.25	308208.6	80.10	0.108	3
Mississippi	35.25	-90.25	2415940.8	471.86	0.061	3
Mississippi	44.75	-92.75	95829.6	21.10	0.118	3
Mississippi	37.75	-89.75	1847179.4	239.50	0.089	3
Mississippi	32.75	-91.25	2953881.3	643.38	0.054	3
Mississippi	44.25	-91.75	153327.3	60.03	0.050	3
Mississippi	38.75	-90.25	444182.9	85.74	0.072	3
Mississippi	39.25	-90.75	443664.9	154.78	0.088	3
Mississippi	45.75	-94.25	30043.9	4.76	0.013	3
Mississippi	30.75	-91.25	2924873.4	507.23	0.065	3
Missouri	44.25	-100.25	630662.1	19.97	0.012	3
Missouri	47.75	-110.75	64099.6	6.26	0.011	3
Missouri	43.25	-98.75	682461.8	22.25	0.012	3
Missouri	47.25	-101.25	469823.8	17.85	0.010	3
Missouri	38.75	-91.25	1357671.7	78.86	0.084	3
Missouri	41.25	-95.75	846301.9	32.60	0.054	3
Missouri	42.25	-96.25	825064.0	27.79	0.032	3
Missouri	39.25	-94.75	1088572.0	37.41	0.073	3
Missouri	46.25	-111.75	37992.5	3.83	0.013	3
Missouri	47.75	-110.25	89041.2	5.48	0.015	3
Missouri	47.75	-106.75	149069.3	8.89	0.012	3
Missouri	48.25	-104.25	237131.5	7.68	0.016	3
Missouri	47.75	-108.75	106155.8	6.88	0.013	3
Murray	-35.22	139.22	1060000.0	7.90	0.024	4
Musi	-2.2	104.56	56700.0	80.40	0.030	4
Nadym	65.6	72.7	48000.0	14.60	0.128	4
Narva	59.75	30.75	278346.0	69.91	0.038	2
Nelson	57.04	-92.3	1132000.0	89.26	0.004	4
Nelson- Saskatchewan	53.75	-101.25	390198.0	30.81	0.012	2
Nemanus	55.02	21.5	98200.0	17.20	0.046	4
Neva	59.48	30.43	282000.0	80.40	0.030	4
Ob	66.6	66.6	2950000.0	404.10	0.073	4
Odra	53.25	14.32	112000.0	16.60	0.370	4
Ohio	37.75	-87.25	251228.8	68.69	0.038	3
Ohio	38.25	-82.75	160579.3	96.74	0.010	3
Ohio	38.75	-85.25	215409.3	67.00	0.045	3
Ohio	40.25	-80.75	64931.0	38.51	0.016	3
Ohio	37.25	-89.25	526026.6	244.42	0.035	3
Olenek	71.8	123.6	198000.0	31.50	0.004	4
Onega	63.8	38.5	12000.0	15.70	0.008	4
Orinocco	8.37	-62.15	1100000.0	1135.00	0.010	4
Panuco	21.59	-98.34	66300.0	17.30	0.016	4
Paraiba Do Sul	-21.45	-41.2	57000.0	30.60	0.010	4
Parana	-34	-58.17	2783000.0	568.00	0.045	4
Pechora	67.6	52.2	312000.0	135.10	0.034	4
Peel	67.37	-134.4	71000.0	24.50	0.006	4
Penzhina	62.28	165.18	71600.0	22.80	0.021	4

Po	44.53	11.39	70000.0	48.90	0.075	4
Potomac	38.9294	-77.1172	29966.3	18.74	0.036	4
Purari	-7.25	145.05	30580.0	84.13	0.002	4
Red	31.25	-91.75	241291.1	70.53	0.033	3
Red	33.75	-96.75	102874.3	4.38	0.020	3
Red	33.75	-94.25	124397.1	15.50	0.017	3
Red	33.75	-97.25	79725.0	7.95	0.068	3
Red	34.25	-98.75	53276.1	1.69	0.017	3
Rhine	51.75	6.25	151811.0	55.86	0.325	2
Rhine	47.25	9.75	6334.6	10.75	0.009	2
Rhine	47.75	8.25	33612.7	31.82	0.039	2
Rhine	47.75	7.75	35691.1	33.04	0.060	2
Rhine	51.52	6.02	224000.0	68.56	0.400	4
Rhone	46.25	6.75	8550.7	12.87	0.014	2
Rhone	46.25	6.25	10688.3	13.70	0.038	2
Rhone	43.92	4.67	95600.0	53.90	0.101	4
Rio Grande	27.75	-105.25	32964.9	0.54	0.253	2
Rio Grande (US)	25.8764	-97.4542	456702.5	0.53	0.030	4
Rio Ica	-2.75	-68.25	157576.3	183.73	0.017	1
Rio Japura	-1.75	-65.75	222517.8	456.86	0.012	1
Rio Jurua	-3.25	-66.25	193108.0	247.97	0.026	1
Rio Jutai	-3.25	-67.25	61586.0	143.68	0.026	1
Rio Madeira	-3.75	-59.25	1454335.0	860.33	0.019	1
Rio Negro	-2.75	-60.75	608636.4	791.74	0.020	1
Rio Purus	-4.25	-61.75	360990.0	431.92	0.034	1
Rufiji	-7.48	37.55	178000.0	35.20	0.010	4
Sacramento	38.35	-121.3	70000.0	20.50	0.030	4
Sacramento	40.75	-122.25	16752.0	6.56	0.015	3
Saint Lawrence			1025000.0	338.25	0.046	4
Sakarya	40.45	30.23	55300.0	5.87	0.160	4
San Joaquin	37.75	-121.25	35058.1	2.83	0.134	3
Santo Antonio do Ica	-3.25	-67.75	1193550.0	1748.67	0.028	1
Schelde	50.75	3.25	11797.7	1.69	0.881	2
Scheldt	51.22	4.15	11400.0	6.00	0.810	4
Seine	49.26	0.26	78600.0	15.80	0.400	4
Severnaya Dvina	64.1	41.9	348000.0	105.60	0.015	4
Seyhan	36.43	34.53	19300.0	4.80	0.010	4
Skagit	48.445	-122.3342	8010.9	14.34	0.010	4
Stikine	56.7081	-132.1303	51592.8	67.69	0.021	4
Susquehanna	40.15	-76.52	71000.0	34.00	0.008	4
Swan Canning	-32	115.9	126021.0	1.31	0.060	4
Tagus	39.75	-3.75	23488.2	0.70	1.572	2
Tana	-2.32	40.31	42000.0	4.75	0.040	4
Tejo	38.44	-9.08	76200.0	9.60	0.148	4
Tennessee	36.75	-88.25	104454.2	27.25	0.022	3
Tennessee	35.25	-88.25	85003.4	42.44	0.021	3
Tennessee	34.75	-85.75	58637.3	23.77	0.013	3

Tennessee	35.75	-84.75	44832.7	14.01	0.013	3
Tocantins	-2.12	-49.3	757000.0	372.00	0.003	4
Tornionjoki	65.48	24.08	39500.0	11.86	0.004	4
Tugela	-29.22	30.5	30112.0	1.10	0.051	4
Uruguay	-33.55	-58.22	240000.0	145.00	0.037	4
Ususmacinta	17.25	-91.3	47700.0	55.52	0.085	4
Vargem						
Grande	-3.25	-68.25	1032887.0	1449.33	0.028	1
Volga	54.75	55.75	109867.0	13.79	0.071	2
Volga			1350000.0	256.50	0.011	4
Weser	53.32	8.34	45800.0	10.60	0.370	4
Wisla	54.06	18.47	198000.0	32.50	0.210	4
Yana	70.8	136	224000.0	32.20	0.006	4
Yellowstone	45.75	-108.75	30548.9	5.51	0.012	3
Yellowstone	45.75	-110.75	9197.0	3.07	0.014	3
Yellowstone	47.75	-104.25	178975.9	9.72	0.014	3
Yenisey	52.25	106.75	444159.0	33.29	0.018	2
Yenisey	50.25	103.75	7844.2	2.75	0.010	2
Yenisey	67.25	86.75	2442750.0	392.12	0.038	2
Yenisey	69.2	86.5	2440000.0	577.30	0.009	4
Yesil	41.24	36.35	35960.0	5.67	0.080	4
Yukon	62.39	-164.48	849000.0	200.00	0.010	4
Zaire	-6.04	12.24	3698000.0	1200.00	0.024	4
Zambezi	-18.55	36.04	1330000.0	106.00	0.010	4
Zhujiang	22.4	113.05	437000.0	363.00	0.014	4

<sup>a</sup> Latitude and longitude are approximate for a number of sites because they are coded to correspond to the center of the half-degree cell in which they fall.

<sup>b</sup> Source code key: 1= CAMREX [Devol et al., 1996], 2= United Nations Global Environmental Monitoring System (GEMS) [2008], 3=Alexander et al. [1996], 4=Harrison et al. [2005]



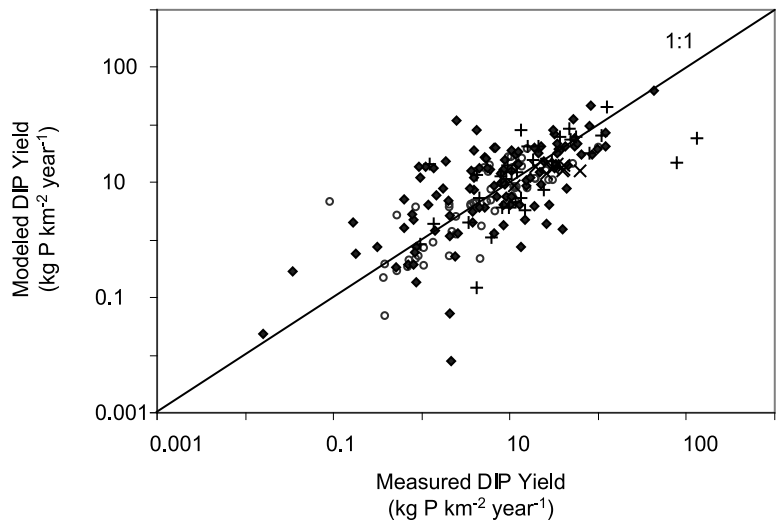
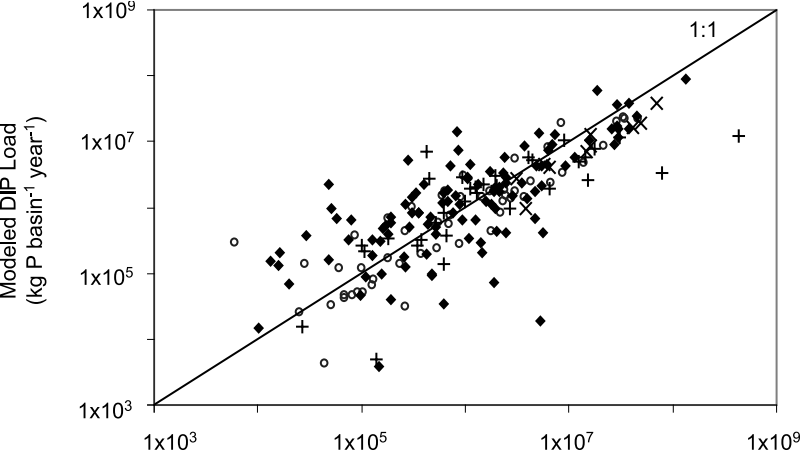
### Data Source

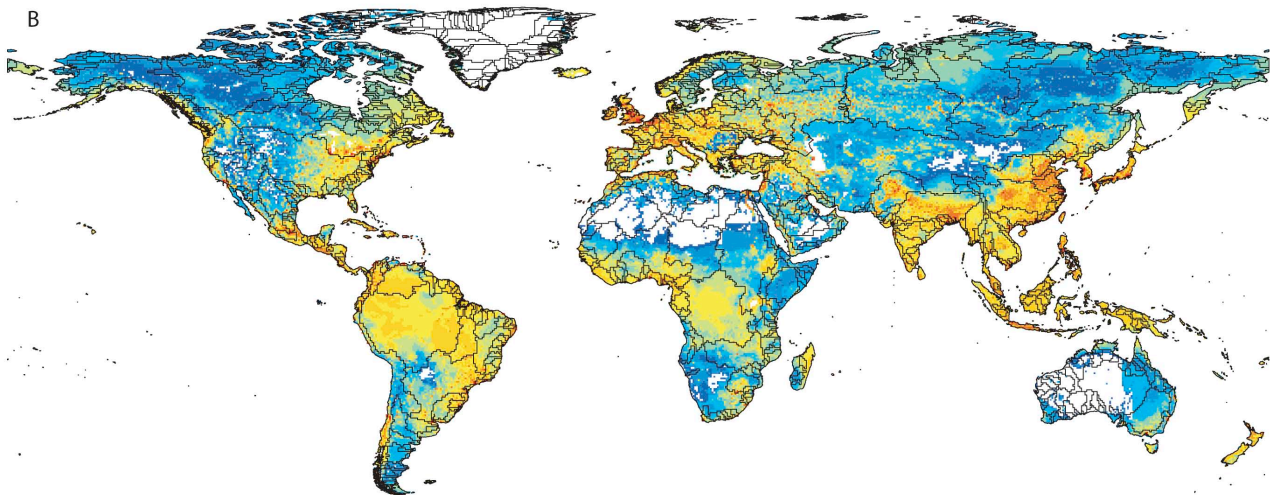
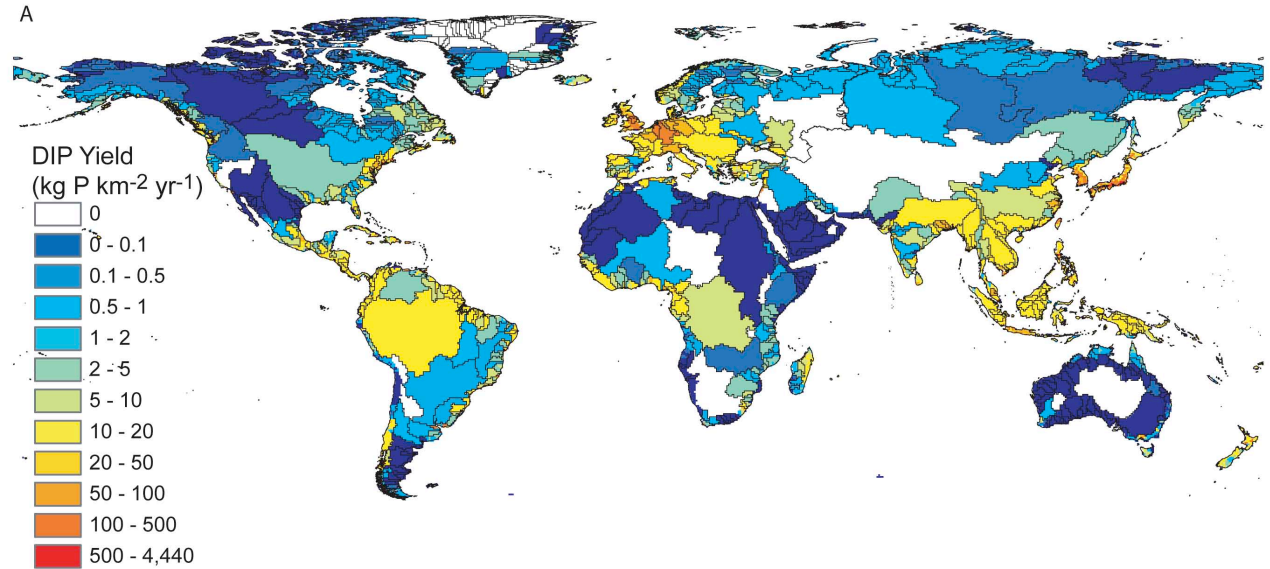
X CAMREX

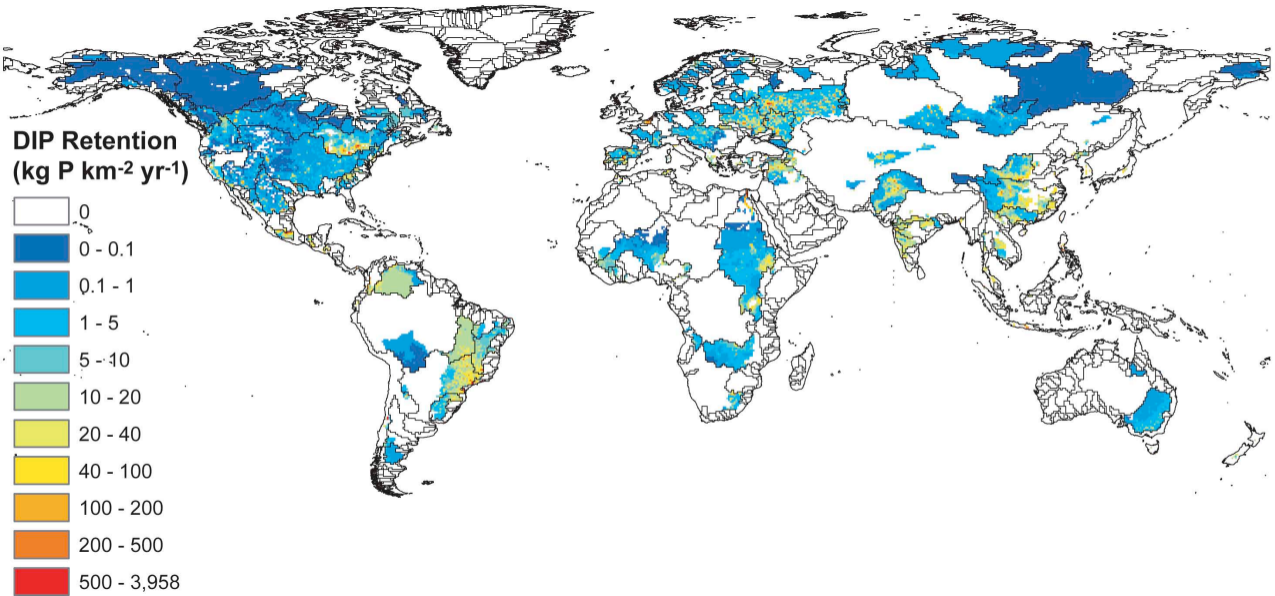
+ GEMS

O USGS-WQN

◆ Harrison et al. (2005)







## Dominant DIP Source

